AGU PUBLICATIONS

JGR

Journal of Geophysical Research: Atmospheres

RESEARCH ARTICLE
10.1002/2014JD022629

Key Points:
- The first UK measurements of $ClNO_2$ using CIMS
- Relationships between N_2O_5 and $ClNO_2$ were dependent on air mass origins
- Cl oxidizes 14.5%, 2.6%, and 25% of alkanes, alkenes, and alkynes

Supporting Information:
- Text S1, and Tables S1 and S2

Correspondence to:
C. J. Percival,
C.Percival@manchester.ac.uk

Citation:
Bannan, T. J., et al. (2015), The first UK measurements of nitryl chloride using a chemical ionization mass spectrometer in central London in the summer of 2012, and an investigation of the role of Cl atom oxidation, *J. Geophys. Res. Atmos.*, *120*, 5638–5657, doi:10.1002/2014JD022629.

Received 2 OCT 2014
Accepted 9 APR 2015
Accepted article online 13 APR 2015
Published online 1 JUN 2015

The first UK measurements of nitryl chloride using a chemical ionization mass spectrometer in central London in the summer of 2012, and an investigation of the role of Cl atom oxidation

Thomas J. Bannan[1], A. Murray Booth[1], Asan Bacak[1], Jennifer B. A. Muller[1], Kimberley E. Leather[1], Michael Le Breton[1], Benjamin Jones[1], Dominique Young[1], Hugh Coe[1], James Allan[1,2], Suzanne Visser[3], Jay G. Slowik[3], Markus Furger[3], André S. H. Prévôt[3], James Lee[4], Rachel E. Dunmore[4], James R. Hopkins[4,5], Jacqueline F. Hamilton[4], Alastair C. Lewis[4,5], Lisa K. Whalley[6,7], Thomas Sharp[6], Daniel Stone[6], Dwayne E. Heard[6,7], Zoë L. Fleming[8], Roland Leigh[9], Dudley E. Shallcross[10], and Carl J. Percival[1]

[1]Centre for Atmospheric Science, School of Earth, Atmospheric and Environmental Science, University of Manchester, Manchester, UK, [2]National Centre for Atmospheric Science, University of Manchester, Manchester, UK, [3]Laboratory of Atmospheric Chemistry, Paul Scherrer Institute, Villigen, Switzerland, [4]Wolfson Atmospheric Chemistry Laboratories, University of York, York, UK, [5]National Centre for Atmospheric Science, University of York, York, UK, [6]School of Chemistry, University of Leeds, Leeds, UK, [7]National Centre for Atmospheric Science, School of Chemistry, University of Leeds, Leeds, UK, [8]National Centre for Atmospheric Science, Department of Chemistry, University of Leicester, Leicester, UK, [9]Department of Physics and Astronomy, University of Leicester, Leicester, UK, [10]Biogeochemistry Research Centre, School of Chemistry, University of Bristol, Bristol, UK

Abstract The first nitryl chloride ($ClNO_2$) measurements in the UK were made during the summer 2012 ClearfLo campaign with a chemical ionization mass spectrometer, utilizing an I^- ionization scheme. Concentrations of $ClNO_2$ exceeded detectable limits (11 ppt) every night with a maximum concentration of 724 ppt. A diurnal profile of $ClNO_2$ peaking between 4 and 5 A.M., decreasing directly after sunrise, was observed. Concentrations of $ClNO_2$ above the detection limit are generally observed between 8 P.M. and 11 A.M. Different ratios of the production of $ClNO_2$:N_2O_5 were observed throughout with both positive and negative correlations between the two species being reported. The photolysis of $ClNO_2$ and a box model utilizing the Master Chemical Mechanism modified to include chlorine chemistry was used to calculate Cl atom concentrations. Simultaneous measurements of hydroxyl radicals (OH) using low pressure laser-induced fluorescence and ozone enabled the relative importance of the oxidation of three groups of measured VOCs (alkanes, alkenes, and alkynes) by OH radicals, Cl atoms, and O_3 to be compared. For the day with the maximum calculated Cl atom concentration, Cl atoms in the early morning were the dominant oxidant for alkanes and, over the entire day, contributed 15%, 3%, and 26% toward the oxidation of alkanes, alkenes, and alkynes, respectively.

1. Introduction

The fate of many anthropogenic trace gas pollutants impacting on health and climate is controlled by chemical oxidation in the troposphere [*Prinn*, 2003]. A rich, complex chemistry influences levels of atmospheric oxidants, with one precursor species, $ClNO_2$, having a potentially important role [*Osthoff et al.*, 2008; *Phillips et al.*, 2012]. $ClNO_2$ releases NO_x and chlorine (Cl) upon photolysis [*Illies and Takacs*, 1977; *Ganske et al.*, 1992] at a time when other oxidants are low, i.e., immediately after sunrise, with *Ghosh et al.* [2011] illustrating that $ClNO_2$ can act as a radical source in the 3–5 h following sunrise. Rate coefficients for reaction of Cl atoms with some volatile organic compounds have been shown to be up to 200 times faster than the comparable reaction with OH. Hence, given a sufficient concentration, this halogen may have an important influence on both air quality and climate [e.g., *Spicer et al.*, 1998], while NO_x is essential for tropospheric ozone production [e.g., *Haagen-Smit and Fox*, 1954].

Laboratory studies have confirmed that heterogeneous uptake of N_2O_5 on aerosols containing chloride produces $ClNO_2$ (R1) [*Finlayson-Pitts et al.*, 1989; *Roberts et al.*, 2009] and ultimately lead to the production of Cl atoms via photolysis (R2) [e.g., *Ganske et al.*, 1992; *Osthoff et al.*, 2008]. However, there are limited field measurements of $ClNO_2$ globally. Measurements from coastal sites [*Osthoff et al.*, 2008; *Kercher et al.*, 2009; *Riedel et al.*, 2012, 2013; *Mielke et al.*, 2013; *Tham et al.*, 2014] and continental settings of Colorado

(USA), Calgary (Canada), and Frankfurt (Germany) by *Thornton et al*. [2010]; *Mielke et al*. [2011], and *Phillips et al*. [2012], respectively, have been recently reported. So far, no such measurements have been made in the UK and in an area that *Sarwar et al*. [2014] predict considerable concentrations of $ClNO_2$ to be formed. Furthermore, the conversion from unreactive sources of chlorine, such as NaCl, to reactive Cl in the troposphere remains uncertain [*Spicer et al*., 1998; *Simpson et al*., 2007].

(R1) $$N_2O_{5(g)} + Cl^-_{(aq)} \rightarrow ClNO_{2(g)} + NO_3{}^-_{(aq)}$$

(R2) $$ClNO_2 + h\nu \rightarrow Cl + NO_2$$

$ClNO_2$ concentrations of more than 1 ppb have been observed on board a ship in the Gulf of Mexico, where plumes originated from both urban and industrial areas [*Osthoff et al*., 2008]. Other measurements on a research vessel have been made by *Riedel et al*. [2012] who saw a maximum of 2.2 ppb in the Los Angeles (LA) region. Recently, *Mielke et al*. [2013] reported measurements of up to 3.6 ppb in LA, again during the Calnex (California Nexus) campaign [*Ryerson et al*., 2013]. *Thornton et al*. [2010] observed up to 450 ppt of $ClNO_2$ inland, 1400 km from the coastline in Boulder, Colorado, which illustrated for the first time that even in the absence of a significant marine source of NaCl, Cl containing aerosols from sources other than marine could lead to $ClNO_2$ production. Vertically resolved $ClNO_2$ measurements from the same region in Colorado by *Riedel et al*. [2013] also illustrated this with mixing ratios of up to 1.3 ppb being observed, reaching levels observed in polluted marine locations. When in an urban plume, *Mielke et al*. [2011] measured concentrations of 100–400 ppt in Calgary, Canada, up to around a half of the levels *Osthoff et al*. [2008] and *Kercher et al*. [2009] observed at polluted coastal sites. Peaks of 800 ppt of $ClNO_2$ were recently observed in mid-continental Europe, and it was suggested that production of $ClNO_2$ in such a setting was expected owing to a strong influence of a marine source of Cl atoms even in continental Europe [*Phillips et al*., 2012]. $ClNO_2$ measurement sites have been generally concentrated around North America, with the exception of *Kercher et al*. [2009] and *Phillips et al*. [2012]. *Sarwar et al*. [2014], however, recently modeled the importance of tropospheric $ClNO_2$ across the northern hemisphere predicting monthly mean nightly maximum concentrations of 400 ppt to be formed in summer in certain areas of western Europe including the UK, with this study also highlighting the importance of seasonality to production.

Osthoff et al. [2008] were the first to document that N_2O_5 was the source of $ClNO_2$ in the field, as illustrated by the positive correlation between them. Since then, *Kercher et al*. [2009], *Thornton et al*. [2010], and *Phillips et al*. [2012] have also documented a positive correlation between the two gaseous species. $ClNO_2$ is relatively unreactive at night, allowing concentrations to build up in the absence of sunlight, and acting as a nighttime sink of NO_x and Cl, but a source of both species upon sunrise [*Osthoff et al*., 2008; *Kercher et al*., 2009; *Thornton et al*., 2010; *Phillips et al*., 2012].

Until recently, Cl-induced oxidation was thought to be of greatest importance in coastal environments and in the marine boundary layer as the primary source of this atom was considered to be production from sea salt [*Keene et al*., 1999]. Sources of Cl for $ClNO_2$ production are not confined to sea salt only [*Mielke et al*., 2011]; likely sources in urban environments are known to be industrial and vehicle combustion providing HCl and aerosol chloride [*Graedel and Keene*, 1995]. Back trajectory modeling completed by the two US studies, *Thornton et al*. [2010] and *Mielke et al*. [2011], suggested that in the absence of a marine influence, the source of Cl in forming $ClNO_2$ is anthropogenic. However, the European study of *Phillips et al*. [2012] disagreed with this stating that very little $ClNO_2$ was produced, even in relatively high N_2O_5 conditions, without a marine influence.

With numerous studies reporting sources of Cl atoms in locations up to an excess of 900 miles away from a marine source [*Thornton et al*., 2010; *Mielke et al*., 2011; *Phillips et al*., 2012], Cl atom-induced oxidation may have a more significant global influence than initially considered, often enhancing tropospheric ozone production [*Simon et al*., 2009; *Sarwar et al*., 2012, 2014]. This release of Cl may be particularly important atmospherically as Cl rate constants for reactions with VOCs are almost exclusively an order of magnitude larger than those of OH. This is particularly so for smaller alkanes which are fairly unreactive with OH.

Phillips et al. [2012] calculated that when a significant amount of $ClNO_2$ is formed, in the few hours following sunrise, the rate of Cl atom production will be greater than the rate of production of OH by O_3 photolysis. This

illustrates the significant role that $ClNO_2$ production and destruction to form Cl atoms may have on the rates of chemical oxidation directly following sunrise, especially as it is at this time when concentrations of other oxidants (OH, NO_3, and O_3) tend to be at a minimum. *Riedel et al*. [2012] suggested that from their measurements made offshore from LA, 25% of total alkane oxidation is driven by Cl atoms, with 45% of the Cl source being from $ClNO_2$ photolysis, in comparison with the oxidation by OH. *Young et al*. [2012] and *Mielke et al*. [2013] also showed that $ClNO_2$ was an important source of Cl atoms in Los Angeles during the 2010 CalNex campaign despite the contribution of Cl from $ClNO_2$ being small in comparison to OH production. Most recently, *Tham et al*. [2014] showed that Cl atom production from fast $ClNO_2$ photolysis exceeded that of OH production from O_3 photolysis by a factor of 3, thus having a significant influence on morning photochemistry in the polluted marine boundary layer of Southern China.

NO_x (NO and NO_2) chemistry influences the oxidizing capacity of the atmosphere, primarily by controlling tropospheric ozone production [e.g., *Crutzen*, 1979]. NO_3 is produced by reaction with NO_2 and O_3 (R4) in both day and night conditions [*Brown et al*., 2006], but in daylight, NO_3 very quickly undergoes photolysis, reproducing O_3 and NO_2. In high levels of NO at the surface, concentrations of NO_3 are likely to be low owing to fast reaction between NO and NO_3. Primarily during the night, NO_3 reacts with NO_2 to form N_2O_5 (R5) [*Wayne et al*., 1991; *Brown et al*., 2003].

The effect of NO_x emissions from urban areas on a global and regional scale depends on its lifetime [*Kercher et al*., 2009]. The NO_x lifetime is fundamentally controlled by nitric acid (HNO_3) production and production of peroxyacyl nitrates (PAN), the latter extending its lifetime and spatial extent. Nitrogen oxides are for the most part removed from the atmosphere via production of nitric acid, via R6 during the day but also R7 at night. Nitric acid is removed from the atmosphere by wet and dry deposition and is regarded as a terminal sink of NO_x [*Finlayson-Pitts and Pitts*, 1999]. Reaction (6) alone is estimated to account for 30–50% of total NO_x removed in polluted urban regions [*Alexander et al*., 2009; *Kercher et al*., 2009]. However, $ClNO_2$ production can disrupt nitric acid formation during the nighttime hours, when N_2O_5 reacts with chloride containing aerosol (R1) instead of with H_2O (R7) and hence limiting the primary method of NO_x removal by HNO_3 formation.

(R3) $$NO + O_3 \rightarrow NO_2 + O_2$$

(R4) $$NO_2 + O_3 \rightarrow NO_3 + O_2$$

(R5) $$NO_3 + NO_2 + M \rightleftarrows N_2O_5 + M$$

(R6) $$NO_2 + OH \rightarrow HNO_3$$

(R7) $$N_2O_5 + H_2O \rightarrow 2HNO_3$$

Here the first measurements of $ClNO_2$ in London, UK, are presented. These measurements took place during July and August 2012, using a chemical ionization mass spectrometer (CIMS) to simultaneously detect both $ClNO_2$ and N_2O_5. Na and Cl measurements were made using a rotating drum impactor (RDI). Measurements of the hydroxyl radical using laser-induced fluorescence at low pressure [*Heard and Pilling*, 2003; *Whalley et al*., 2010], and a comprehensive suite of supporting measurements, for example of speciated VOCs, ozone, and photolysis frequencies, enabled the relative contribution of Cl atoms to the oxidation of VOCs compared with OH and O_3 to be evaluated.

2. Experimental

2.1. Site Description

The summer intensive observation period as part of the ClearfLo (Clean Air for London) campaign (http://www.clearflo.ac.uk/) were made in North Kensington, London, between the 20th of July and 19th of August 2012. This is an urban background site located at 51.52 N, 0.21 W, based in the grounds of the Sion Manning School. This school is situated within a residential area of London situated 7 km west of Central London. Colocated is an air quality monitoring station run by the Automatic Urban and Rural Network; details of which are documented in *Bigi and Harrison* [2010], which present an overview of hourly data of CO, NO, NO_2, SO_2, and PM_{10} between the years of 1996–2008.

The ClearfLo project fundamentally aims to provide long-term combined atmospheric measurements, resulting in a greater accuracy for future atmospheric predictions, specifically within the city of London.

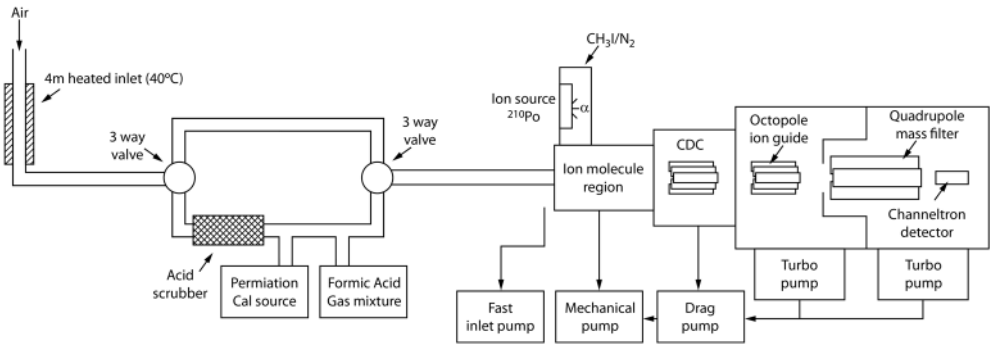

Figure 1. Schematic of the CIMS instrument.

For this project, a large suite of instrumentation, comprising both ground and airborne measurements, with meteorological, gas, and aerosol phase measurements, is combined. The range of chemical species measured at a number of locations, coupled with the extensive urban network of measurements (NO_x, CO, particles, and in many cases O_3) already in place, is intended to provide a database that can be used to improve urban models.

Measurements were primarily taken during two approximately 1 month long intensive observation periods, one in the winter (January–February 2012) and the second in summer (July–August 2012). $ClNO_2$ was however not measured in the winter. The second campaign, discussed here, ran during the period of the 2012 Olympic Games and provided an opportunity to assess how such a large event in a city affects important atmospheric species, although this is not the focus of this paper. An overview of the ClearfLo project is given by *Bohnenstengel et al*. [2014].

2.2. Analytical Techniques

2.2.1. Chemical Ionization Mass Spectrometry

A chemical ionization mass spectrometer (CIMS) was used to make measurements of $ClNO_2$ and N_2O_5, at a frequency of 1 Hz. The CIMS was constructed and designed by the Georgia Institute of Technology and has been described in detail by *Nowak et al*. [2007] (see also the schematic in Figure 1). Briefly, the CIMS detects trace gasses in the atmosphere by selectively ionizing specific molecules and then detects ions using mass spectrometry [*Nowak et al*., 2007]. Detailed description of the instrument and its operation can be found in *Bannan et al*. [2014].

The ion molecule chemistry using iodide ions (I^-) to detect N_2O_5 as NO_3^- ($m/z = 62$) has been described in detail by *Le Breton et al*. [2014a] and was also employed for measurements of N_2O_5 in this study. *Le Breton et al*. [2014a] illustrated the reliability of this method after intercomparison with the broadband cavity enhanced absorption spectrometer (BBCEAS). *Wang et al*. [2014] suggested that the use of *m/z* 62 is prone to interferences from species such as PAN, HO_2NO_2, and HNO_3 and use *m/z* 62 to measure the sum of N_2O_5 and NO_3 with their thermal dissociation-CIMS. The setup of our ion optics, inlet, and ionization system in our "cold" CIMS does not allow detection of NO_3, as found from numerous laboratory calibrations. Possible interferences from HNO_3 at both atmospherically relevant and very high concentrations *m/z* 62 have been extensively studied in the laboratory, and no evidence for this has been observed. Possible interferences from PAN or HO_2NO_2 at *m/z* 62 have not been specifically checked for this work; however, both absolute concentrations and time series against the BBCEAS when intercomparison projects have been run, such as *Le Breton et al*. [2014a], show very good agreement in N_2O_5 measurements. Such interferences are therefore not deemed important here.

$ClNO_2$ was measured at the mass $I.ClNO_2$ (*m/z* 207.9) as in *Phillips et al*. [2012]. Formic acid and nitric acid, which were utilized for relative calibration of $ClNO_2$ and N_2O_5, were detected at *m/z* 173 and *m/z* 189 [*Bannan et al*., 2014; *Le Breton et al*., 2014b].

The methyl iodide reagent ions were produced as previously described by *Le Breton et al*. [2012], from a gas mixture which comprised 0.5% methyl iodide [CH_3I (99.5%, Sigma-Aldrich), H_2O (0.5%) in N_2 (99.998%, BOC)]. The CH_3I mixture and N_2 (99.998%, BOC), at flow rates of 1 sccm and 1.5 slm, respectively, are passed over the

alpha emitting radioactive source (Polonium-210 inline ionizer, NRDinc Static Solutions Limited) creating an excess of I^- and I. $(H_2O)^-$ in the ionization region which react with the species of interest for detection.

2.2.1.1. Calibrations, Sensitivity, and Limit of Detection of the CIMS

The final calibration of the CIMS was completed post campaign for both N_2O_5 and $ClNO_2$, relative to formic acid, which was calibrated and measured throughout the campaign. This relative calibration has been successfully utilized by *Le Breton et al*. [2014a] for N_2O_5. It is assumed that the ratio between formic acid and $ClNO_2$ sensitivity remains a constant throughout. Formic and nitric acid calibrations were run twice daily to ensure a stable sensitivity over time, with sensitivities of 1.2 and 0.84 ion counts ppt^{-1}, respectively (Bannan et al., in prep). The 3σ limit of detection (LOD) for formic acid was calculated to be 34 ppt.

Calibration of N_2O_5 was completed by flowing dry N_2 over solid purified N_2O_5 into the CIMS and a NO_x analyzer (Thermo Fisher, model 42i NO–NO_2–NO_x Analyzer), with the concentration determined by the stoichiometric ratio of NO_2:N_2O_5, in R5. The flow of N_2O_5 is separated into two flows, one to the CIMS and the other to the NO_x analyzer. The N_2O_5 passing into the NO_x analyzer is thermally decomposed to produce NO_2 and NO_3, of which NO_2 is then detected. Detailed description of which can be found in *Le Breton et al*. [2014a]. There have been reported instances where NO_3 is sensitive on the NO_x analyzer, thus influencing the concentrations of N_2O_5 that are reported in this study. However, numerous intercomparisons with the BBCEAS, also independently measuring N_2O_5, as in *Le Breton et al.* [2014a], show that this calibration method works well, producing very good agreements in total concentrations reported. The possible interference of NO_3 on the NO_x analyzer is therefore not deemed important in terms of our reported concentrations.

The solid N_2O_5 was prepared by the gas phase reaction of NO_2 and O_3, R4 and R5. Details of procedure, while ensuring that the N_2O_5 was of the highest purification possible, are detailed in *Le Breton et al*. [2014a] which include numerous purification steps. Water vapor was excluded from this procedure by first flushing the system with O_3 for 20 min prior to the introduction of NO_2 and using dry nitrogen in the calibration flows. These measures were taken in order to reduce the production of HNO_3 as an impurity as much as possible. During calibration, HNO_3 was simultaneously measured by the CIMS throughout. It was found that only up to 7% of the sample was found to be nitric acid; thus, the possible interference of HNO_3 on observed NO_x on the Thermo 42i was negligible.

(R4) $$NO_2 + O_3 \rightarrow NO_3 + O_2$$

(R5) $$NO_3 + NO_2 + M \rightleftarrows N_2O_5 + M$$

$ClNO_2$ was produced by flowing 1 slm of a known concentration of N_2O_5 in dry N_2 through a wetted NaCl scrubber, which is dispersed on the surface of 25 cm tubing with a 2.2 cm OD as well as on the surface thin of nylon filings to increase surface area for R1 to take place. The conversion of N_2O_5 to $ClNO_2$ has been shown to have a 100% conversion yield as a result of the reaction with NaCl [*Finlayson-Pitts et al*., 1989] and is an assumption made here. The loss of N_2O_5 signal, i.e., loss of a known concentration of N_2O_5, in comparison with the gain of $ClNO_2$ was used to determine our sensitivity to $ClNO_2$, a process used in *Osthoff et al*. [2008] and *Kercher et al*. [2009].

The ionization efficiency and thus sensitivity of the CIMS has been previously shown to be dependent on the counts per second of $I.H_2O^-$, which is dependent on the relative humidity of the sample [*Slusher et al*., 2004]. As illustrated in *Le Breton et al*. [2014a], above a threshold of 100,000 cps of $I.H_2O^-$, the sensitivity to formic acid is independent of relative humidity with the tuning of our system. Due to the linearity between formic and N_2O_5 sensitivities at varying $I.H_2O$ cps, it is assumed that the independent threshold for N_2O_5 is also 100,000 cps of $I.H_2O^-$, as described by *Le Breton et al*. [2014a]. This assumption was also made for the $ClNO_2$ measurements. Throughout the ClearfLo measurement period, the average $I.H_2O^-$ was in excess of 400,000 cps, well above the threshold required for sensitivity independent of changes in water vapor. This was achieved through the tuning of the ion optics and introduction of H_2O into the ionization mix. It is therefore concluded that the measurements during this period are independent of ambient relative humidity changes.

The sensitivity of the system for N_2O_5 and $ClNO_2$ was 1.09 and 0.093 counts ppt^{-1}, respectively, throughout the ClearfLo campaign. The 3σ $ClNO_2$ and N_2O_5 LOD during the summer ClearfLo campaign was 11 and 4 ppt, respectively, when calculated over a 30 s averaging period. Using the error in the individual slope of the calibrations results in a total uncertainty of 30%.

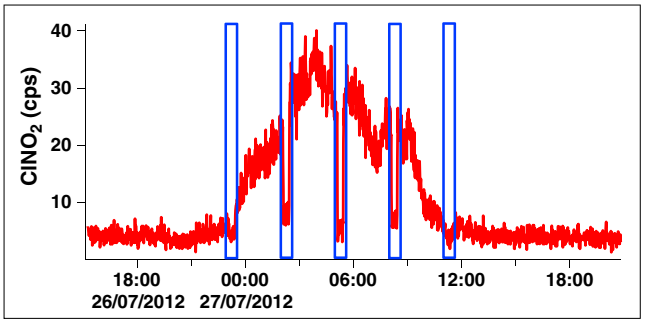

Figure 2. Raw counts of $ClNO_2$ on the 27th of July 2012. Backgrounds at 11 P.M., 2 A.M., 5 A.M., 7 A.M., and 10 A.M. (UTC) indicated by the boxed regions illustrate the effectiveness of the sodium bicarbonate-covered nylon filings acting as the scrubber. Data here are averaged to 5 s.

Figure 2 illustrates that the sodium bicarbonate scrubber efficiently removed the majority of $ClNO_2$ during background measurements. However, in times of high nighttime production, background levels obtained using the installed scrubber were not sufficient to remove all $ClNO_2$ signals to instrumental background; therefore, daytime counts, which have a very low background, were used in data analysis and calculation of the LOD.

On the 19th and 20th of July 2012, mass scans were set to automatically run every 30 min during nighttime hours between 200 and 210 amu with a step change of 0.05 amu, to determine the exact mass speak of $ClNO_2$. Upon analysis of these mass scans, a value of 207.9 was determined and used throughout the campaign, agreeing with the previous laboratory calibrations. Complete spectral scans from 0 to 300 amu were automatically taken every 2 h throughout the campaign. Analysis of these regularly ensured that the system was stable and ensured the peaks were assigned correctly, although no variation in the *m/z* axis was observed.

Numerous tests and preventative measures were employed throughout the campaign to ensure that $ClNO_2$ measurements remain unaffected by the inlet in use and that N_2O_5 was not being converted to $ClNO_2$ on the inlet walls. A heated inlet, held at 40°C, was used in conjunction with a very low residence time of 0.3 s and ensured reaction time here was at a minimum. A total flow rate of 35 slm in sample mode ensured that residence time in the inlet was minimal. During periods of high N_2O_5 concentrations and in the absence of $ClNO_2$, there was no difference between the raw counts of sample mode and background mode, i.e., no increase in $ClNO_2$ as a result of an increase of N_2O_5, suggesting no conversion on the inlet walls is taking place. This can be illustrated during one 20 min background on the night of the 17th of August where the raw counts of $ClNO_2$ at *m/z* 207.9 were 3.15 ± 1.02 cps and the following 20 min in sample mode that gave raw counts of 3.42 ± 1.41 cps at a time when significant N_2O_5 concentrations were present (229 ± 13 ppt). On this night, enhancements of $ClNO_2$ rarely exceeded the limit of detection, but significant peaks of 500 ppt of N_2O_5 were recorded with an average of 285 ppt. Inlet conversion of N_2O_5 to $ClNO_2$ would be greatest at the end of the campaign during these periods of high N_2O_5; however, no evidence for this was observed.

Furthermore, throughout the campaign, there were periods when N_2O_5 dropped below the LOD and $ClNO_2$ remained constant, again showing that there was no conversion of N_2O_5 to $ClNO_2$ on the inlet walls. This is illustrated during periods such as on the 1st of August at 05:00–05:30 where an N_2O_5 signal below that of the limit of detection was observed and a concentration of 95 ppt of $ClNO_2$ was observed during this period.

The CIMS monitored 11 masses with a dwell time of 100 ms. One second data from sampling and calibration cycles are averaged to 30 s. Correlation with meteorological data is completed with 5 min averaged data. Backgrounds were applied using daily averages. Using this approach, a maximum error of ±8 ppt was estimated for the reported nighttime concentrations.

2.2.2. Rotating Drum Impactor (RDI)

Aerosols were sampled with a rotating drum impactor with a 2 h time resolution in three aerodynamic diameter size fractions (0.3–1.0, 1.0–2.5, and 2.5–10 μm). The particle containing air is sampled through the instrument with a flow rate of $1\ m^3\ h^{-1}$. Size segregation results when the particles pass through three rectangular nozzles of decreasing size. The particles are deposited by impaction on Apiezon-coated polypropylene foils mounted on aluminum wheels. After each 2 h sampling interval, the wheels automatically rotate stepwise to a blank section of the foil before a new sampling interval takes place.

Trace elemental composition in the aerosol samples was determined with synchrotron radiation-induced X-ray fluorescence spectrometry at the X05DA beamline [*Flechsig et al.*, 2009] at the Swiss Light Source at

the Paul Scherrer Institute, Villigen PSI, CH. Kα lines of the elements with atomic number $Z = 11–30$ (Na–Zn) were measured. Further details of the sampling and analysis of the trace elements can be found in *Visser et al*. [2014] and in previous application examples including *Bukowiecki et al*. [2010] and *Richard et al*. [2011].

Na, because of the lack of other major sources than marine, is used as an indicator of marine influence acting on the site at any one time. Because of the very high correlation between the Cl and Na ($R^2 = 0.97$ for size fractions 1.0–2.5 and 2.5–10 μm) throughout the whole measurement period, it can be assumed that the vast majority of the chloride containing aerosol during the summer measurement period is of a marine source.

2.2.3. Hydroxyl Radical Measurements

OH radical concentrations were measured by laser-induced fluorescence spectroscopy at low pressure, using the so-called FAGE (fluorescence assay by gas expansion) technique [*Heard and Pilling*, 2003]. The instrument is described in detail in *Whalley et al*. [2010], and only a brief overview is given here. An air-conditioned converted shipping container housed the FAGE instrument, with the OH fluorescence cell located within a weather-proof enclosure on the container roof, with feedthroughs for a pumping line and signal/control electronics. OH is excited at ~308 nm via the $Q_1(1)$ transition of the OH ($A^2\Sigma^+$, $v' = 0 - X^2\Pi_i$, $v'' = 0$) band using a 5 kHz pulse repetition frequency YAG pumped titanium sapphire laser. The subsequent fluorescence, also at ~308 nm, is collected by a fast-lens arrangement, passed through a narrow-band interference filter, and focused onto the photocathode of a channel photomultiplier, which is switched off during the laser pulse and whose output is processed via a photon counter. The photon counter uses two integration gates to enable the contribution from any solar-scattered radiation and dark counts to be accounted for, and tuning the laser wavelength on and off the OH line center enables the contribution from laser-scattered light to be subtracted. Air was sampled through a 1 mm diameter pinhole into a fluorescence cell held at 1.1 Torr, and a fast-flow rate through the cell was achieved using a Roots blower backed by a rotary pump. The sampling pinhole was 3.5 m above the ground and ~10 m horizontally away from the CIMS instrument for $ClNO_2$ measurements in the Manchester container. The instrument was calibrated in the field using photolysis at 185 nm of a known concentration of water vapor in zero air within a turbulent flow tube to generate OH, with the product of the photon flux at 185 nm and the water vapor photolysis residence time measured using a chemical actinometer. The average sensitivity of the instrument, obtained from this calibration was $C(OH) = 1.56 \times 10^{-7}$ cts s^{-1} $molecule^{-1}$ cm^3 mW^{-1}, from which a detection limit of 3.8×10^5 molecule cm^{-3} was obtained for a typical laser power of 12 mW, signal-to-noise ratio of 1, and averaging period of 200 s. The measurements were recorded with 1 s time resolution, and the accuracy of the measurements was ~26%.

2.2.4. VOC Measurements

VOC measurements were obtained using two gas chromatography (GC) instruments. The volatile fraction of VOCs (C_2–C_7 hydrocarbons, with a small selection of OVOCs) was measured using a dual channel (DC)-GC-FID, while a comprehensive two dimensional GC (GC × GC-FID) measured the less volatile fraction (C_6–C_{13}, with a large group of OVOCs). The DC-GC-FID instrument and calibration setup is described in detail in *Hopkins et al*. [2003]. The GC × GC-FID is composed of an Agilent 7890 GC (equipped with a splitless injector and FID operating at 200 Hz, Agilent Technologies, Wilmington, DE, USA), Markes TT24-7 thermal desorption unit (with an air server attachment, Markes International, Llantrisant, UK),and a total transfer flow modulator (6-port, 2-way diaphragm valve modulator, Valco Instruments, Houston, TX, USA) actuated using a solenoid valve and controlled by "in house" software. The GC × GC-FID setup is described in detail in *Lidster et al*. [2011]. Calibrations on both instruments were performed at regular intervals using a gas standard with 30 ozone precursor species (NPL30, National Physical Laboratory, Teddington, UK).

2.2.5. NO_x Measurements

NO and NO_2 data were taken using an Air Quality Design custom built high sensitivity chemiluminescence analyzer with blue light NO_2 converter. The instrument consists of two channels measuring NO by reaction with excess O_3 to form excited state NO_2, followed by the detection of the resultant chemiluminescence. The air flow in one of the channels first passes through a photolytic converter where light at 395 nm photolysis NO_2 to NO. Calibration of the instrument is done every 2 days using 5 ppm NO in nitrogen cylinder (BOC certified to NPL scale), diluted to ~20 ppb using scrubbed zero air (BOC BTCA 178). The NO_2 conversion efficiency was calibrated using gas phase titration of the NO standard by O_3. NO_y data were taken using TEI 42i TL NO analyzer with molybdenum converter.

2.2.6. Photolysis Rate Measurements

Actinic fluxes of solar radiation were measured using a Metcon spectral radiometer [*Edwards and Monks*, 2003] and were used to calculate the photolysis frequencies of a number of trace gasses, including NO_2 $j(NO_2)$. $j(NO_2)$ was calculated from actinic flux measured with a 2Π receiver optic with a horizontal shadow ring which provides a measure of the downwelling flux in one hemisphere. The spectral radiometer was operated at ground level. Under these conditions, upwelling radiation can be neglected [*Hofzumahaus et al*., 1999], as the low ground albedo or reflectivity has a negligible impact on the calculated photolysis rates (we expect this to be the case for all photolabile compounds). $J(ClNO_2)$ was scaled to this measurement, as described in the next section.

3. Modeling

A box model was used to calculate Cl atom concentrations during the campaign so that the rate of oxidation of VOCs by Cl atoms could be compared with oxidation by measured OH and measured ozone. The model contained part of the Master Chemical Mechanism v3.2 [*Jenkin et al*., 2012] which in its entirety treats the degradation of 135 VOCs following oxidation by OH, O_3, and NO_3, and for alkanes only, oxidation by Cl atoms, and contains ~6700 species and ~17,000 reactions. Complete details of the kinetic and photochemical data used in the mechanism are available at the MCM website (MCM; http://mcm.leeds.ac.uk/MCM/). Here a subset of the MCM was used which contained the Cl atom oxidation of 11 measured alkanes (C1–C8) by H atom abstraction to form HCl:

(R9) $$Cl + RH \rightarrow HCl + R$$

The MCM does not contain a mechanism for the Cl atom-initiated oxidation of alkenes (C2–C5) or alkynes (acetylene), which were also measured during the campaign. Reactions of Cl atoms with these measured species were added to the MCM v3.2 mechanism using rate coefficients taken from the NIST database [*Manion et al*., 2014]. Rate constants for the additional Cl atom reactions that are included in the model are detailed in Table S2 in the supporting information. For H-atom abstraction channels, the reported yield was used to generate HCl, but for other channels, for example, the addition to double or triple bonds, the reaction was treated as a simple loss for Cl atoms, with no recycling of Cl atoms, for example, by photolysis of any intermediates. In addition, reaction of Cl atoms with model generated organic intermediates was not considered. This is in contrast with the initial oxidation by OH and O_3 which proceeds completely to water vapor and CO_2. The model does not contain an inorganic mechanism for chlorine, and so the following gas phase reactions were added as outlined by *Riedel et al*. [2014], including the thermal decomposition of $ClONO_2$ [*Anderson and Fahey*, 1990].

(R2) $$ClNO_2 + h\nu \rightarrow Cl + NO_2$$

(R10) $$HCl + OH \rightarrow Cl + H_2O$$

(R11) $$Cl + O_3 \rightarrow ClO + O_2$$

(R12) $$ClO + NO_2 \rightarrow ClONO_2$$

(R13) $$ClO + HO_2 \rightarrow HOCl + O_2$$

(R14) $$ClO + NO \rightarrow Cl + NO_2$$

(R15) $$ClONO_2 + h\nu \rightarrow Cl + NO_3$$

(R16) $$ClONO_2 + h\nu \rightarrow ClO + NO_2$$

(R17) $$ClONO_2 + M \rightarrow ClO + NO_2 + M$$

(R18) $$HOCl + h\nu \rightarrow Cl + OH$$

$J(ClNO_2)$ was calculated using the Tropospheric Ultraviolet and Visible Radiation Model, version 4.1, and then scaled to measured $J(NO_2)$ using a surface albedo of 0.0. This approach, as used in *Stone et al*. [2010], allows for variation in solar radiation, as affected by cloud cover, to be accounted in the photolysis rates.

The only source of Cl atoms considered in the model was the initial photolysis of $ClNO_2$, and hence, HCl and other gas phase inorganic Cl species in the reaction mechanism described earlier are only generated by the

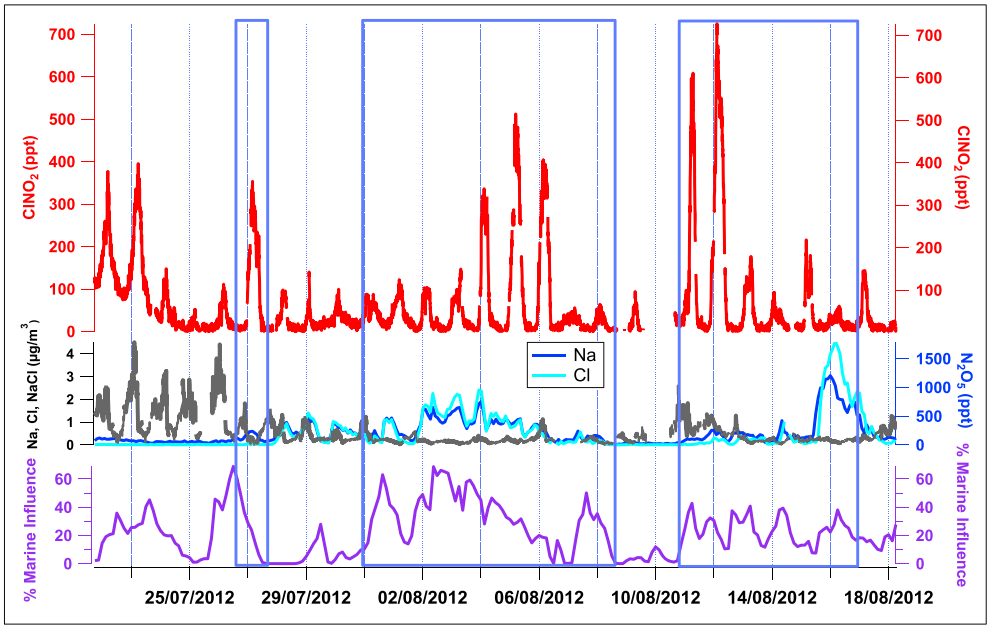

Figure 3. Complete time series of $ClNO_2$, N_2O_5, Na ($PM_{2.5-1.0} + PM_{10-2.5}$), and Cl ($PM_{1-0.3} + PM_{2.5-1.0} + PM_{10-2.5}$), and % marine influence during the summer ClearfLo campaign. Purple trace shows percentage of the air masses originating from a marine origin, as defined by NAME modeling. Blue boxes indicate air masses primarily defined by a marine influence, and blank areas are air masses primarily of a continental dominance.

model with an assumed initial concentration of zero. Chlorine atom concentrations were then calculated by the box model using a Facsimile integrator [*Curtis and Sweetenham*, 1987] and constrained with comeasured concentrations of VOCs, NO_x, HO_2, and O_3 photolysis frequencies and other species. The model was integrated forward for 10 days after which time a diurnal steady state Cl atom concentration was reached, with the peak Cl atom concentration varying by less than 1%. Further details regarding the box model methodology can be found in *Whalley et al*. [2010].

4. Results and Discussion

Complete time series of $ClNO_2$, N_2O_5, Na, and Cl are shown in Figure 3, illustrating that $ClNO_2$ was detected every night of the campaign. A mean nighttime, i.e., sunset to sunrise, $ClNO_2$ concentration of 84 ppt was observed and a maximum peak of 724 ppt at 2:55 A.M. on the 12 of August 2014, from 1 min averaged data. $ClNO_2$ measured results are comparable with those made by *Phillips et al*. [2012], with $ClNO_2$ peaks of 750 ppt. Peak concentrations of $ClNO_2$ are 40% smaller than those reported by *Osthoff et al*. [2008] but 60% larger than peaks reported in Colorado by *Thornton et al*. [2010], almost certainly as a result of the measurement locations. Mean nightly maximum concentrations of 207 ppt are reported, around half of what was predicted for parts of Western Europe in summer by *Sarwar et al*. [2014]. Increased concentrations of chloride aerosol generally coincide with air masses of a predominantly marine origin (Figure 3). A large chloride containing aerosol concentration does not, however, directly translate into enhanced $ClNO_2$ production. Likewise, a large amount of N_2O_5 does not continuously mean an enhanced production of $ClNO_2$.

4.1. Diurnal Profile of $ClNO_2$ and Daytime Peaks

A very distinct pattern is observed in the daily $ClNO_2$ production and destruction (Figure 4), similar to that of previous studies [*Osthoff et al*., 2008; *Kercher et al*., 2009; *Thornton et al*., 2010; *Mielke et al*., 2011]. $ClNO_2$ signal above that of the limit of detection was measured, on average, until 11 A.M. and only exceed detectable limits after sunset (LOD = 11 ppt), consistent with $ClNO_2$ being produced in the absence of sunlight. In nighttime hours, a gradual build-up of $ClNO_2$ is observed and concentrations increase until sunrise, at which point concentrations decrease rapidly. The average values for the mean diurnal cycle range between below the

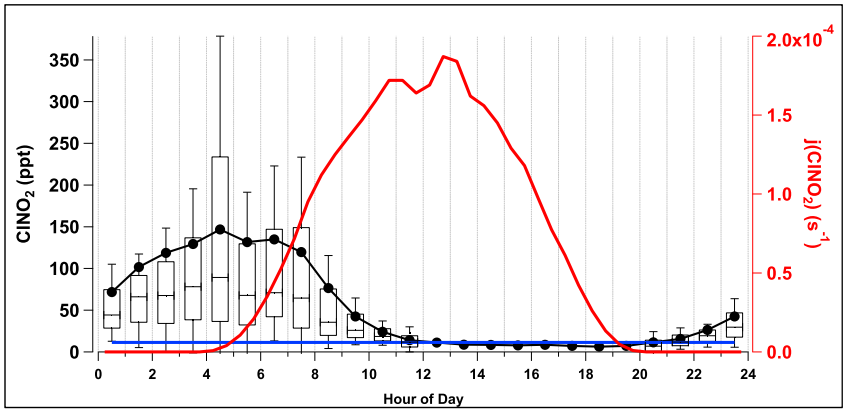

Figure 4. Average diurnal cycle of $ClNO_2$ and solar radiation for the 27 days of summer ClearfLo. The box and whisker plots show the median, and 5th and 95th percentiles of $ClNO_2$, with the solid black circles with connecting lines illustrating the mean values. Data between 12 A.M. and 8 A.M. whose mean values are below the LOD (signified by the blue line) are excluded from statistical analysis. Red line illustrates j($ClNO_2$).

LOD and 150 ppt with peaks in $ClNO_2$ concentrations being seen between 4 A.M. and 5 A.M., just prior to sunrise at approximately 5 A.M. (local time).

In keeping with the work of *Phillips et al.* [2012], the $ClNO_2$ mass that was recorded (*m/z* 207.9) has a very low daytime background, agreeing well with the expectation that no $ClNO_2$ would be observed at these times. However, there are two examples when small peaks of $ClNO_2$ are observed soon after sunrise, as illustrated in Figure 5. Here following the nights of the 30th July and 2nd August 2012, increases in $ClNO_2$ concentrations are observed after sunrise, a result that has not previously been reported. N_2O_5 measurements do not, however, reflect this pattern. Such daytime peaks only occur very soon after sunrise, at a time when the daily solar radiation and thus photolysis rates are at their lowest. Such daytime peaks are unlikely to be produced as this time but from movement of air parcels from a region of higher concentrations of $ClNO_2$, possibly higher in the troposphere where emissions of NO are reduced and N_2O_5 concentrations are likely to be enhanced in comparison to ground level.

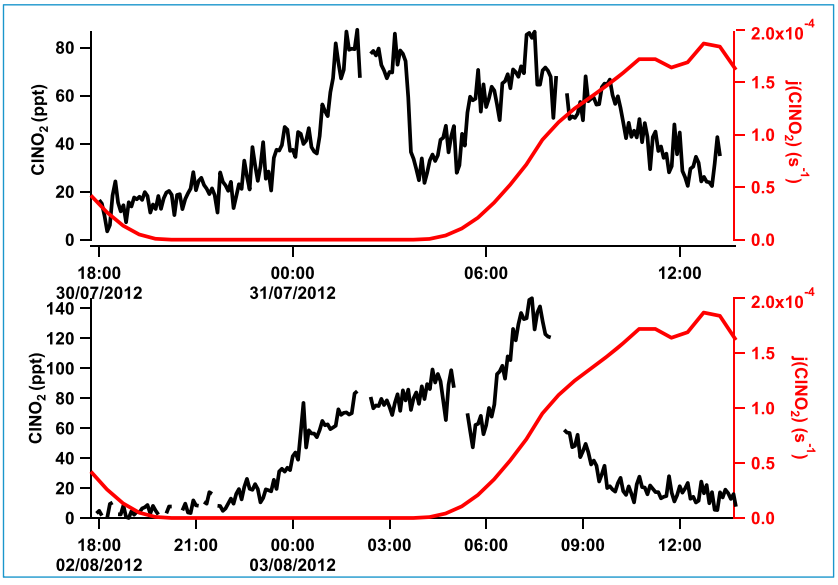

Figure 5. Post-sunrise peaks of $ClNO_2$ on the nights of the 30th of July and 2nd of August. Black trace indicates $ClNO_2$ concentration, and red shows j($ClNO_2$).

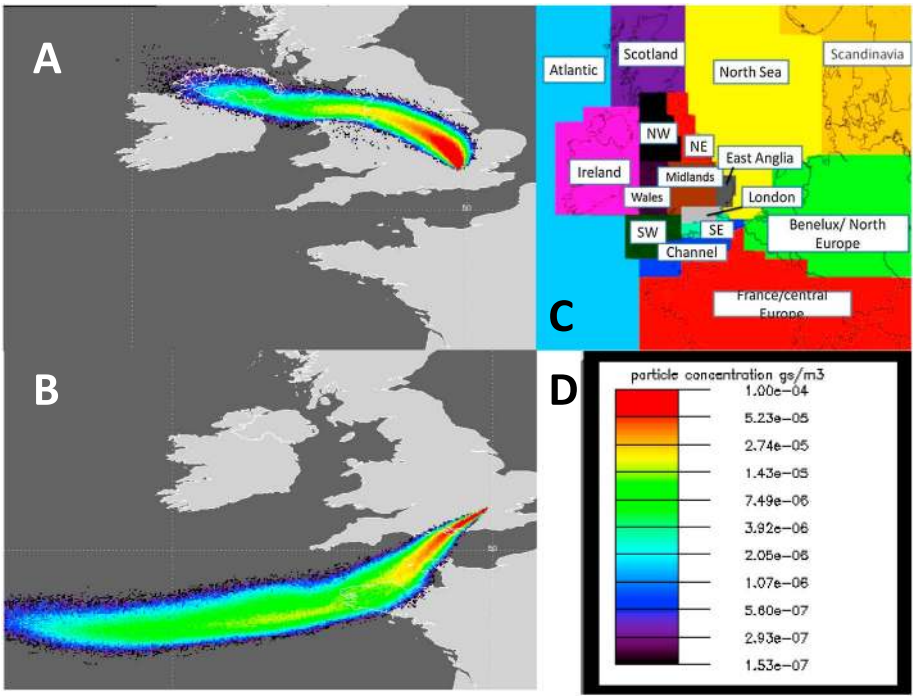

Figure 6. (a) 28th July (6:00) and (b) 21st August (21:00) are examples of continental and marine periods. (c) A map of the regional division used to define marine and continental is shown. (d) Scale of particle concentration for Figures 6A and 6B.

An average $ClNO_2$ lifetime was also calculated using the slope of the decrease of the average diurnal profile of $ClNO_2$ against time to get the loss rate, assuming no change in air mass had occurred. Decreases in the concentration of $ClNO_2$ are also occasionally observed during the nighttime hours, at a time when photolysis cannot be the removal mechanism, e.g., specifically on 28th, 29th, and 30th of July. Nocturnal $ClNO_2$ removal pathways have generally been reported to be negligible, with $ClNO_2$ being assumed to be relatively inert [*Wilkins et al*., 1974; *Frenzel et al*., 1998; *Rossi*, 2003; *Osthoff et al*., 2008]; however, the work of *Roberts et al*. [2008] and *Kim et al*. [2014] would suggest that this may not be strictly true. Nighttime removal mechanisms are not, however, observed in the average diurnal cycle, and for this reason, observed losses are attributed solely to photolysis, with $J(ClNO_2)$ controlling the lifetime. Using this methodology, an average lifetime of $ClNO_2$ of 2.6 ± 0.23 h is calculated, within the range reported by previous studies [e.g., *Ganske et al*., 1992; *Ghosh et al*., 2011].

4.2. Meteorological and Chemical Regimes

Dispersion modeling was carried out using the UK Met Office's Numerical Atmospheric-dispersion Modelling Environment (NAME) dispersion model [*Jones et al*., 2007]; see detail in *Bohnenstengel et al*. [2014]. The NAME dispersion model was used to produce three hourly averaged air mass footprints for the campaign period that track the air mass origins during the previous 24 h. More details are included in the supporting information. A count of particle concentration was taken every 15 min during the 24 h period and summed together to create a probability footprint, highlighting the number of particles traveling through pre-defined regions including UK continental, Atlantic Ocean, the Channel, the North Sea, and continental Europe (see Figure 6 and examples of continental and marine air masses) that reach the measurement site. For each three hourly footprint, the total amount of particles counted in each region was translated into a % regional influence (from the total particle count in the whole domain).

To quantify the extent of the marine influence during each three hourly period, the Atlantic Ocean, the Channel, and the North Sea were combined, resulting in a % marine influence as shown in Figure 3. This represents the amount of time the air mass has spent over marine areas, irrespective of which continental regions it has also passed over before or after the marine surface.

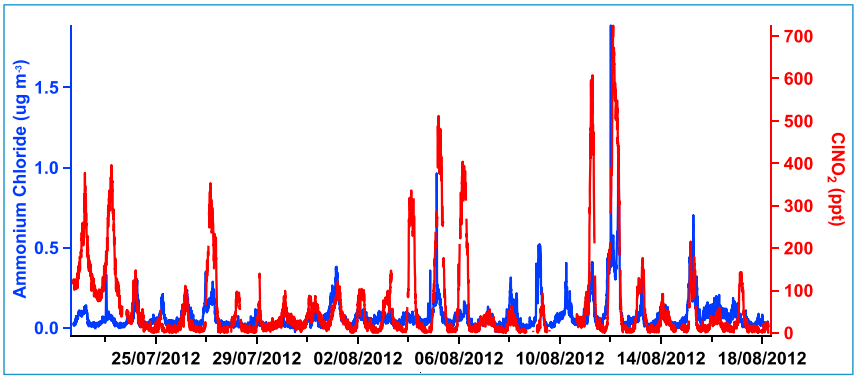

Figure 7. $ClNO_2$ and primary ammonium chloride aerosol concentrations.

Using gas phase and aerosol data, as well as NAME dispersion modeling, it is possible to separate the time series into two different regimes: marine and continental. A classification of either a continental or marine dominance is illustrated in Figure 3 with blue boxes around the marine periods and in Table S1 in the supporting information. In this study, we will define a marine influenced air mass as above the 15% marine as defined by NAME, as it is at this level when a general enhancement of Na is observed in the RDI analysis. As can be seen in this figure, Na and Cl aerosol concentrations are generally highest during marine-dominated regimes, while N_2O_5 concentrations are significantly lower than average. The converse is generally true under continental regimes where measured N_2O_5 concentrations are high and Na and Cl aerosol measurements are comparatively low.

4.3. $ClNO_2$:N_2O_5 Ratios

In keeping with the work of *Osthoff et al*. [2008], *Mielke et al*. [2011], and *Phillips et al*. [2012], there are large differences in concentrations of $ClNO_2$ each night as well as relative production rates of $ClNO_2$:N_2O_5. *Phillips et al*. [2012] showed that the concentration ratio of $ClNO_2$ to N_2O_5 varied by over an order of magnitude from 3:1 to 0.2:1, similar to that reported by *Thornton et al*. [2010]. Two ratios are calculated for this study, one using peak values from nighttime concentrations and another from mean nighttime values. When using average nighttime concentrations, ratios of $ClNO_2$:N_2O_5 ranged from 0.017:1 to 2.4:1 with a mean of 0.51:1. Nighttime peak concentration values give a range of 0.04:1 to 3.6:1 and a mean ratio of 0.72:1. The daily $ClNO_2$:N_2O_5 ratios are included in Table S1 in the supporting information.

In this location and time, $ClNO_2$ production is generally limited to $ClNO_2$:N_2O_5 ratios of less than 1:1 with the exception of the 3rd and 4th of August, closer to the lower ratio values reported by *Phillips et al*. [2012]. The mean ratio for the defined continental conditions is calculated to be 0.15:1, in comparison with 0.74:1 in the defined marine regime, suggestive that an enhanced marine source of aerosol chloride increased $ClNO_2$ production.

The diurnal profile of particulate ammonium chloride and its peaks in nighttime concentration show a similar structure to measured $ClNO_2$, as shown in Figure 7. Ammonium chloride measurements were performed using an Aerodyne High-Resolution Time-of-Flight Aerosol Mass Spectrometer. Details regarding this instrument and data analysis can be found in *Young et al*. [2014]. The correlation with ammonium chloride suggests that a number of sources of chloride could be of importance to $ClNO_2$ production. It should, however, be noted that the NH_4Cl peaks at night are most likely due to a temperature effect (semivolatile repartitioning to gaseous NH_3 and HCl during the day), so the day-night modulation is probably not related to the production of $ClNO_2$; however, it does not rule out the possibility of this particulate chloride acting as a precursor to $ClNO_2$ production.

4.4. Relationship Between N_2O_5 and $ClNO_2$

$ClNO_2$ concentrations show a large variability each night as well as relative production rates of $ClNO_2$:N_2O_5. Also reported here is the variability in the relationship between production and loss of $ClNO_2$ and N_2O_5.

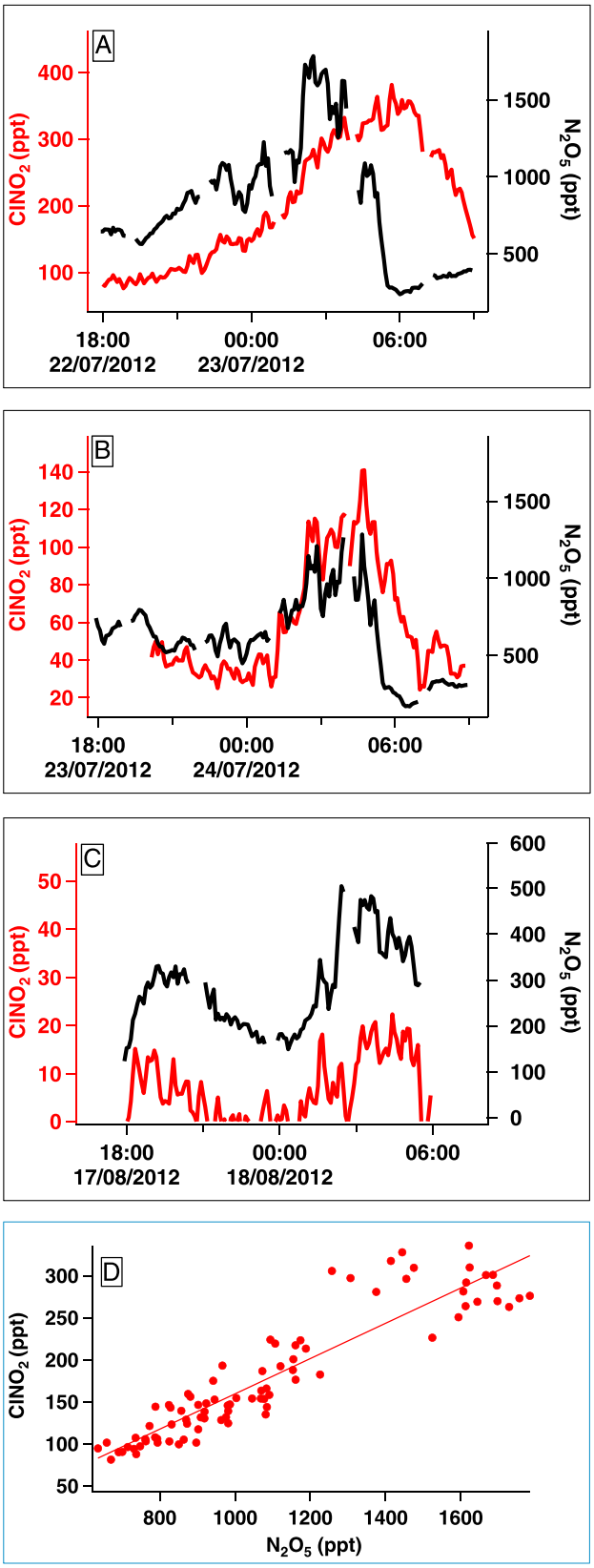

Studies concurrently measuring N_2O_5 and $ClNO_2$ have generally reported that as N_2O_5 increases, $ClNO_2$ also increases [*Osthoff et al.*, 2008; *Kercher et al.*, 2009; *Thornton et al.*, 2010; *Phillips et al.*, 2012]. This is to be expected, as increasing the reactants increases the products of such reactions (R1). However, in this study, the nighttime relationship between N_2O_5 and $ClNO_2$ varies as well as the ratio between the two (Table S1). A positive correlation between the two gaseous species is observed for certain parts of the study as shown in Figure 8. This concurs with studies such as *Phillips et al.* [2012], but there are noticeably different regimes where $ClNO_2$ and N_2O_5 anti-correlate (Figure 8).

Figure 8 and Table S1 illustrate that N_2O_5 and $ClNO_2$ regularly positively correlate in predominantly continental air masses. In such conditions, N_2O_5 concentrations are some of the highest measured during the campaign, while Na and Cl concentrations are small, i.e., little marine influence. Negative correlations between N_2O_5 and $ClNO_2$ are also observed as seen in Figure 9. This relationship is often associated with marine define air mass, which is generally defined by high chloride containing aerosol and low N_2O_5. This is, however, not true of every night, and there are examples where neither a positive nor negative relationship is observed. The positive and negative relationships that have been described are not exclusively defined by the regimes presented, and this classification approach is not always valid.

The continental and marine regimes can be inspected using a very simple model

Figure 8. (a–c) Three examples of nighttime relationships between $ClNO_2$ and N_2O_5. All examples here are defined as primarily continental air masses with predominantly continental England and/or Europe influence. 22rd and 23th of July corresponded to some air masses primarily from continental England. On the night of the 17th of August, the air masses were primarily of a European continental influence. Figure 8d shows the linear relationship between N_2O_5 and $ClNO_2$ for the night of the 22nd inclusive of hours 8 P.M. to 4 A.M.

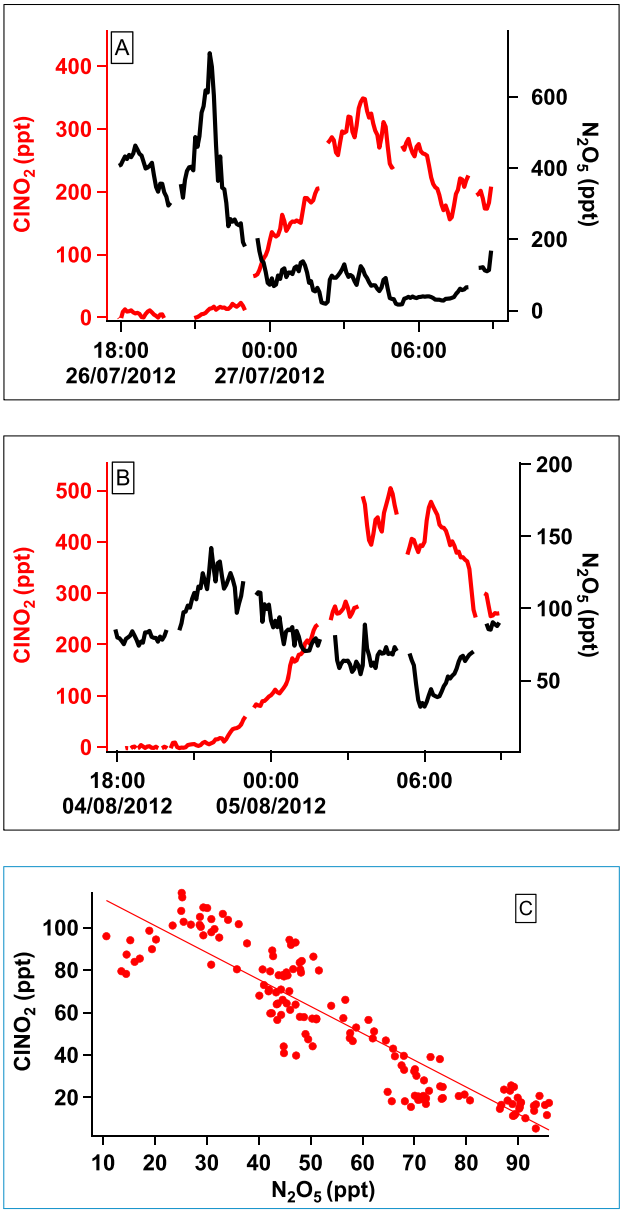

Figure 9. (a and b) Two examples of nighttime relationships between $ClNO_2$ and N_2O_5. On the night of the 26th of July, there was a big marine influence from the northwest, i.e., the North Sea. On the night of the 4th of August, the English Channel provides the majority of the air mass. Figure 8c shows strong linear negative correlation between N_2O_5 and $ClNO_2$ on the 31st of July 2012 (between 6 P.M. and 9 A.M.). All case studies here are defined by air primarily of a marine origin. Please note differences in concentration scales.

that includes both N_2O_5 and $ClNO_2$ production and using the steady state approximation, assuming the following reactions govern the production of $ClNO_2$.

(R4) $NO_2 + O_3 \rightarrow NO_3$

(R5) $NO_3 + NO_2 \rightleftarrows N_2O_5$

(R19) $N_2O_5 + \text{aerosol}_{NaCl} \rightarrow ClNO_2$

Here it should be noted that k_{R19} is a composite rate coefficient and that no attempt is made to model the detailed microphysics of this system; we are merely interested to know whether a change in available $[Cl^-]$, here modeled as [NaCl] for which we have measurements for, can alter the correlation between N_2O_5 and $ClNO_2$. The size-segregated Na and Cl data of the two larger size fractions ($PM_{2.5-1.0} + PM_{10-2.5}$) are added to total PM_{10} concentrations to give total NaCl concentrations. Throughout the measurement campaign, the R^2 between the Cl and Na was 0.97. This shows that the addition of the two species is a fairly reliable method for detecting sea salt given the limited sources of both species other than marine in the supermicron fraction (note that this is only valid for measurement locations strongly influenced by marine air masses).

We are well aware that conversion of N_2O_5 to $ClNO_2$ occurs over a range of $[Cl^-]$ and indeed much lower than that corresponding to pure NaCl [*Bertram and Thornton*, 2009; *Roberts et al.*, 2009]. We also note that *Osthoff et al.* [2008] show that reactions of N_2O_5 can take place on all aerosol particles, with uptake efficiencies dependent on water content, presence of organic coating, and nitrate and chloride concentrations and that the efficiency of $ClNO_2$ formation depends on chloride concentration. We note that NaCl is unlikely to have enough surface area and often do not have enough total chloride to provide the observed $ClNO_2$ and that HCl for example may well be a more important source whenever sea salt-derived aerosol mixes with urban pollution. Nevertheless, the basic question we seek to answer using the simplest of models is whether a change in $[Cl^-]$ can give rise to the change in correlation observed.

By increasing the concentrations of $[Cl^-]$ via NaCl within this simple model, N_2O_5 versus $ClNO_2$ will first correlate (Figure 10a) and finally switch to an anti-correlation as concentrations of Cl^- (NaCl) increase (Figure 10b). NaCl concentrations used to produce these modeled results are based on values observed.

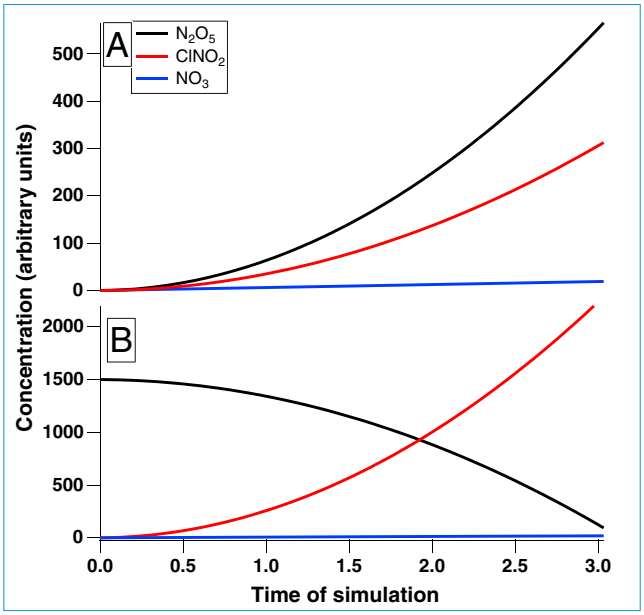

Figure 10. Simulation of the relationship between N_2O_5 and $ClNO_2$ under different NaCl concentrations. (a) NaCl set 0.31 μg m^{-3}. (b) NaCl set 2.63 μg m^{-3}. Please note arbitrary units for time and concentration of species.

For this, values from the 22nd of July and the 14th of August are used where Na + Cl peak at 0.31 and 2.63 μg m^{-3}, respectively, and are used to represent the continental and marine regimes, respectively. Figure 10 shows that the relationship between $ClNO_2$ and N_2O_5 first is positively correlated, and then as the NaCl loading increased, a negative correlation between the two emerges. This in effect is recreating the marine versus continental regimes but does not take into consideration a change in N_2O_5 concentrations. As Figure 10 illustrates, the relationship between N_2O_5 and $ClNO_2$ is reproduced qualitatively by this simple model, especially so for the positive and negative correlations, but we have made no attempt to model the detailed microphysics of the heterogeneous process and simply used a fixed rate coefficient for R19. The point of this exercise is to investigate whether the change in correlation can be explained by different NaCl loadings (really $[Cl^-]$), and at this first approximation, it can.

4.5. Calculation of Relative Oxidation Rates of Alkanes, Alkenes, and Alkynes by Reaction With OH, O_3, and Cl Atoms

The total rates of removal of alkanes, alkenes, and alkynes by reaction with the oxidants OH, O_3, or Cl atoms at a given time during the campaign were calculated using the following:

$$-\mathrm{d[alkanes]}/\mathrm{d}t = [\mathrm{X}]\sum_i k_{\mathrm{X+alkane},i}[\mathrm{alkane},i] \quad (1)$$

$$-\mathrm{d[alkenes]}/\mathrm{d}t = [\mathrm{X}]\sum_i k_{\mathrm{X+alkene},i}[\mathrm{alkene},i] \quad (2)$$

$$-\mathrm{d[alkynes]}/\mathrm{d}t = [\mathrm{X}]\sum_i k_{\mathrm{X+alkyne},i}[\mathrm{alkyne},i] \quad (3)$$

where [X] is the concentration of measured OH, measured O_3, or Cl atoms calculated using the MCM at a given time in the campaign, and [alkane,*i*], [alkene,*i*], and [alkyne,*i*] represent the corresponding measured speciated concentration of each alkane, alkene, and alkyne, and k_X is the individual bimolecular rate coefficient for the reaction of X with each species at the measured pressure and temperature. Rate coefficients were taken from those used in the MCM [*Jenkin et al.*, 1997; *Saunders et al.*, 2003] or from the NIST database [*Manion et al.*, 2014].

For this study, two model runs for London were performed using this method. In the first run, the time series of the Cl atom concentration was calculated for 12th August 2008, during which the $ClNO_2$ concentration was the highest observed during the campaign (724 ppt at ~3 A.M.; Figure 3). In the second run, the diurnal variation of $[ClNO_2]$ averaged for the entire campaign was used to drive the production of Cl atoms in the model. For both runs, the campaign-averaged diurnal concentrations for [OH], $[O_3]$, and VOCs were used to calculate the rates of oxidation. The OH concentration measured by FAGE, the measured O_3 concentration, and the Cl atom concentration calculated using the MCM are shown in Figure 11.

It can be seen that Cl atom concentrations rise rapidly after sunrise (5 A.M. local time), as expected given their source being $ClNO_2$ photolysis, peaking around 6 A.M. local time, and for 12th August,

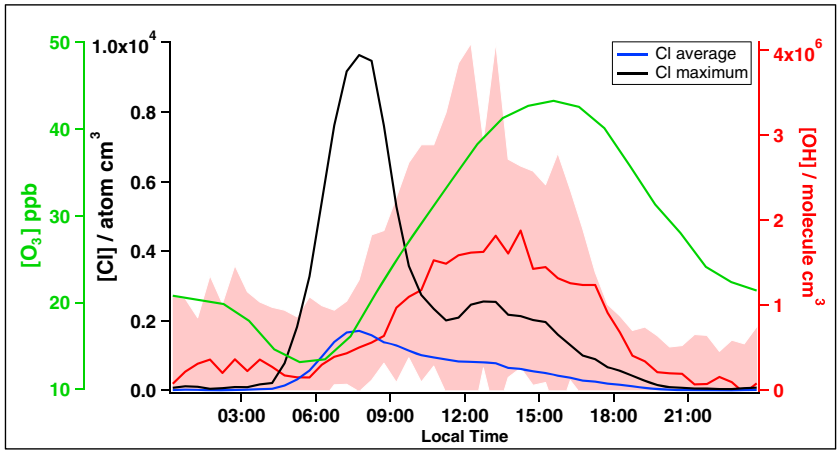

Figure 11. Cl atom concentration profile calculated for 12th August 2012 (black), during which the maximum observed concentration of $ClNO_2$ was observed; Cl atom concentration profile calculated as an average for the entire campaign (blue); and the measured OH concentration averaged for the entire campaign (red), together with the 1σ day to day variability of the OH data used to generate the average diurnal profile (light red shading). Campaign-averaged measured O_3 concentration is also included (green).

concentrations reached ~0.95×10^4 atoms cm^3, which is about 150 times lower than the average peak concentration of OH, which occurs around solar noon. This peak Cl atom concentration is approximately 10 times lower than calculated in Los Angeles during the CALNEX study [*Riedel et al.*, 2014], reflecting the lower $ClNO_2$ concentration observed in London (peak of 724 ppt) compared to Los Angeles (~1500 ppt). Any differences in the model photolysis rates and overall Cl reactivity from the two cities will also impact the steady state Cl atom concentration predicted. Although $ClNO_2$ concentrations in this study are very low by noon, Cl atoms are recycled via reactions ((R2), (R10)–(R18)) and do not reach zero again until later in the afternoon. The chemical turnover rates for the oxidation of the sum of measured alkanes, alkenes, and alkynes by reaction with OH, O_3, or Cl atoms, as calculated by equations (1)–(3) are shown in Figure 12 for 12th August, when Cl atoms peaked, and in Figure 13 for the average behavior of all oxidants over the campaign.

By summing the oxidation rate across the entire 24 h period shown in Figures 12 and 13, the total % removed by reaction with the three oxidants for each type of VOC was calculated and is shown in Table 1.

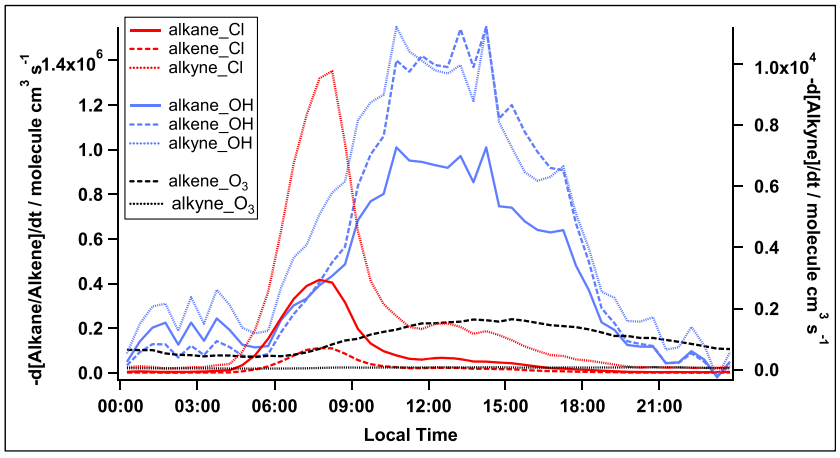

Figure 12. Rate of removal of alkanes, alkenes, and alkynes by reaction with the oxidants OH (measured, campaign average), O_3 (measured, campaign average), and Cl atoms calculated for 12th August 2012, when the calculated Cl atom concentration was at its maximum.

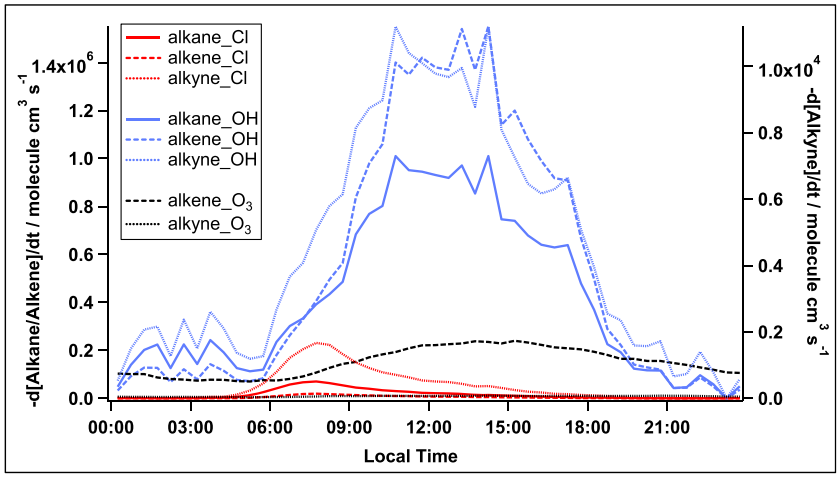

Figure 13. Rate of removal of alkanes, alkenes, and alkynes by reaction with the oxidants OH (measured), O_3 (measured), and Cl atoms (calculated), all averaged over the entire campaign.

The % removal by Cl atoms for tailpipe emissions, Boston, and LA was again determined using equations (1)–(3), and using NIST kinetic data [*Manion et al.*, 2014] but using the mean Cl atom concentration from the campaign average, but calculated using steady state approximations. For these calculations, rather than using the MCM to calculate Cl atom concentrations, they were calculated using a simple steady state expression with the Cl atom production rate estimated from the observed loss rate of $ClNO_2$ and removal of Cl atoms via reaction with the VOC concentrations from each environment. Regeneration of Cl atoms via R2, R10 through R18 were not considered. Final calculations of % influence were made using the mean diurnal profile of measured O_3 and OH, with the result also included in Table 1.

From Table 1, it can be seen that although OH is the dominant oxidant in London during the summer ClearfLo campaign, Cl atoms on average remove ~4%, 1%, and 7% of alkanes, alkenes, and alkynes, respectively, which is significant. For 12th August, when Cl atoms were calculated to be at a maximum, Cl atoms removed ~15%, 3%, and 26% of these species and in the early morning are the dominant oxidants for alkanes.

Outputs from the MCM agree well with the calculations of the Tailpipe, Boston, and LA environments, despite a much more simplistic approach for the latter. In comparison with the London average, MCM calculations show a slightly smaller impact in terms of alkane oxidation by Cl but larger in terms of the alkene. Using both of these approaches has illustrated that neglecting the contributions made by Cl atoms will significantly underestimate the degree of chemical processing of VOCs in central London and the other environments that have been calculated in this study.

Table 1. Relative Importance of Cl, OH, and O_3 to the Oxidation of Three Groups of VOCs From Both Tailpipe Emissions and Cities Around the World[a]

	Tailpipe	Boston	LA	London (12/8/12)	London Average
Alkane Cl%	8.49	8.49	9.91	15.28	3.72
Alkane OH%	91.51	91.51	90.09	84.72	96.28
Alkane O_3%	–	–	–	–	–
Alkene Cl%	0.50	0.31	0.30	2.82	0.66
Alkene OH%	43.67	32.99	31.26	76.19	77.89
Alkene O_3%	55.83	66.70	68.44	20.99	21.45
Alkyne Cl%	7.52	8.70	8.70	26.21	7.38
Alkyne OH%	77.02	89.70	89.70	72.79	91.38
Alkyne O_3%	15.46	1.60	1.60	1.00	1.24

[a]VOC concentration data used for the calculations for Boston [*AQIRP*, 1995], tailpipe [*Simmons and Burridge*, 1981; *Cullen*, 1993; *Stevenson et al.*, 1998], and LA [*Fraser et al.*, 1997] are included as well as for London, using measured VOC data. See text for details of calculations.

5. Conclusions

Significant nighttime concentrations of up to 724 ppt of $ClNO_2$ during the summer ClearfLo campaign in summer 2012 have been observed, and mean nighttime concentrations of 84 ppt suggest that production of this species is a common occurrence in Central London. The average diurnal profile of $ClNO_2$ saw an increase directly after sunset and increased until sunrise at approximately 5 A.M. at which point photolysis occurred. $ClNO_2$ concentrations on average reached a level below that of the LOD around 11 A.M. On two occasions, however, an early morning rise in $ClNO_2$ concentrations was observed after sunrise, a feature previously not reported.

A marine source of chloride is deemed to be the most important source of chloride aerosol for the production of $ClNO_2$, based on the higher $ClNO_2$:N_2O_5 production ratios during periods when Na and Cl concentrations are high. Both positive and negative correlations between $ClNO_2$ and N_2O_5 are observed, and the cause was inspected using a very simple model. This model showed that the change in relationship can potentially be explained by different loadings of chloride containing aerosol.

Despite OH being the dominant oxidant, Cl has been shown to have a significant affect. Cl atoms on average remove ~4%, 1%, and 7% of alkanes, alkenes, and alkynes, respectively, but removed ~15%, 3%, and 26% of these species following the night of greatest $ClNO_2$ production (724 ppt). Results suggest that neglecting the contributions made by Cl atoms will underestimate the degree of chemical processing of VOCs in central London, Boston, LA, and from tailpipe emissions.

Here the first ever measurements of $ClNO_2$ in the UK have been reported, as well as their effect on total VOC oxidation in numerous scenarios. Further measurement studies in different local conditions and environments in the UK as well as globally are important. Extensive modeling must also be carried out to further understand how the Cl released from $ClNO_2$ photolysis affects the overall oxidizing capacity of the atmosphere.

Acknowledgments
This work was supported by NERC (NE/H003193/1), the Swiss National Science Foundation (SNFS grants 200021_132467/1 and 200020_150056/1), and the UK Met Office's NAME model. Please email Thomas Bannan at Thomas.bannan@manchester.ac.uk for all the data used here.

References

Alexander, B., M. G. Hastings, D. J. Allman, J. Dachs, J. A. Thornton, and S. A. Kunasek (2009), Quantifying atmospheric nitrate formation pathways based on a global model of the oxygen isotopic composition ($\Delta^{17}O$) of atmospheric nitrate, *Atmos. Chem. Phys.*, *9*, 5043–5056, doi:10.5194/acp-9-5043-2009.

Anderson, L. C., and D. W. Fahey (1990), Studies with nitryl hypochlorite: Thermal dissociation rate and catalytic conversion to nitric oxide using an NO/O_3 chemiluminescence detector, *J. Phys. Chem.*, *94*(2), 644–652, doi:10.1021/j100365a027.

AQIRP (1995), Effects of gasoline T50, T90 and sulfur on exhaust emissions of current and future technology vehicles. Auto/Oil Air Quality Improvement Research Program, Technical Bulletin No. 18.

Bannan, T. J., A. Bacak, J. Muller, A. M. Booth, B. Jones, M. Le Breton, K. E. Leather, P. Xiao, D. E. Shallcross, and C. J. Percival (2014), Importance of direct anthropogenic emissions of formic acid measured by a chemical ionisation mass spectrometer (CIMS) during the Winter ClearfLo Campaign in London, January 2012, *Atmos. Environ.*, *83*, 301–310, doi:10.1016/j.atmosenv.2013.10.029.

Bertram, T. H., and J. A. Thornton (2009), Toward a general parameterization of N_2O_5 reactivity on aqueous particles: The competing effects of particle liquid water, nitrate and chloride, *Atmos. Chem. Phys.*, *9*(21), 8351–8363, doi:10.5194/acp-9-8351-2009.

Bigi, A., and R. M. Harrison (2010), Analysis of the air pollution climate at a central urban background site, *Atmos. Environ.*, *44*(16), 2004–2012, doi:10.1016/j.atmosenv.2010.02.028.

Bohnenstengel, S. I., et al. (2014), Meteorology, air quality and health in London: The ClearfLo project, *Bull. Am. Meteorol. Soc.*, *11*(5), 1913–1928.

Brown, S. S., H. Stark, and A. R. Ravishankara (2003), Applicability of the steady state approximation to the interpretation of atmospheric observations of NO_3 and N_2O_5, *J. Geophys. Res.*, *108*(D17), 4539, doi:10.1029/2003JD003407.

Brown, S. S., et al. (2006), Nocturnal odd-oxygen budget and its implications for ozone loss in the lower troposphere, *Geophys. Res. Lett.*, *33*, L08801, doi:10.1029/2006GL025900.

Bukowiecki, N., P. Lienemann, M. Hill, M. Furger, A. Richard, F. Amato, A. S. H. Prévôt, U. Baltensperger, B. Buchmann, and R. Gehrig (2010), PM10 emission factors for non-exhaust particles generated by road traffic in an urban street canyon and along a freeway in Switzerland, *Atmos. Environ.*, *44*(19), 2330–2340, doi:10.1016/j.atmosenv.2010.03.039.

Crutzen, P. J. (1979), The role of NO and NO_2 in the chemistry of the troposphere and stratosphere, *Annu. Rev. Earth Planet. Sci.*, *7*, 443–472.

Cullen, M. J. P. (1993), The unified forecast/climate model, *Meteorol. Mag.*, *122*(1449), 81–94.

Curtis, A. R., and W. P. Sweetenham (1987), *Facsimile/Chekmat User's Manual*, edited by AERER12805, Her majesty's stn. off, Norwich, England.

Edwards, G. D., and P. S. Monks (2003), Performance of a single-monochromator diode array spectroradiometer for the determination of actinic flux and atmospheric photolysis frequencies, *J. Geophys. Res.*, *108*(D16), 8546, doi:10.1029/2002JD002844.

Finlayson-Pitts, B. J., and J. N. Pitts Jr. (1999), *Chemistry of the Upper and Lower Atmosphere: Theory, Experiments, and Applications*, Academic Press, San Diego, Calif.

Finlayson-Pitts, B. J., M. J. Ezell, and J. N. Pitts (1989), Formation of chemically active chlorine compounds by reactions of atmospheric NaCl particles with gaseous N_2O_5 and $ClONO_2$, *Nature*, *337*(6204), 241–244, doi:10.1038/337241a0.

Flechsig, U., A. Jaggi, S. Spielmann, H. A. Padmore, and A. A. MacDowell (2009), The optics beamline at the Swiss Light Source, *Nucl. Instrum. Methods Phys. Res., Sect. A*, *609*(2), 281–285.

Fraser, M. P., G. R. Cass, B. R. Simoneit, and R. A. Rasmussen (1997), Air quality model evaluation data for organics. 4. C2–C36 non-aromatic hydrocarbons, *Environ. Sci. Technol.*, *31*(8), 2356–2367, doi:10.1021/es960980g.

Frenzel, A., V. Scheer, R. Sikorski, C. George, W. Behnke, and C. Zetzsch (1998), Heterogeneous interconversion reactions of $BrNO_2$, $ClNO_2$, Br_2, and Cl_2, *J. Phys. Chem. A*, *102*(8), 1329–1337, doi:10.1021/jp973044b.

Ganske, J. A., N. Berko, and B. J. Finlayson-Pitts (1992), Absorption cross sections for gaseous $ClNO_2$ and Cl_2 at 298 K: Potential organic oxidant source in the marine troposphere, *J. Geophys. Res.*, *97*, 7651–7656, doi:10.1029/92JD00414.

Ghosh, B., D. K. Papanastasiou, R. K. Talukdar, J. M. Roberts, and J. B. Burkholder (2011), Nitryl chloride (ClNO2): UV/Vis absorption spectrum between 210 and 296 K and O (3P) quantum yield at 193 and 248 nm, *J. Phys. Chem. A*, *116*(24), 5796–5805, doi:10.1021/jp207389y.

Graedel, T. E., and W. C. Keene (1995), Tropospheric budget of reactive chlorine, *Global Biogeochem. Cycles*, *9*(1), 47–77, doi:10.1029/94GB03103.

Haagen-Smit, A. J., and M. M. Fox (1954), Photochemical ozone formation with hydrocarbons and automobile exhaust, *J. Air Pollut. Control Assoc.*, *4*, 105–109, doi:10.1080/00966665.1954.10467649.

Heard, D. E., and M. J. Pilling (2003), Measurement of OH and HO_2 in the troposphere, *Chem. Rev.*, *103*(12), 5163–5198.

Hofzumahaus, A., A. Kraus, and M. Müller (1999), Solar actinic flux spectroradiometry: A technique for measuring photolysis frequencies in the atmosphere, *Appl. Opt.*, *38*(21), 4443–4460.

Hopkins, J. R., A. C. Lewis, and K. A. Read (2003), A two-column method for long-term monitoring of non-methane hydrocarbons (NMHCs) and oxygenated volatile organic compounds (o-VOCs), *J. Environ. Monit.*, *5*, 8–13, doi:10.1039/b202798d.

Illies, A. J., and G. A. Takacs (1977), Gas phase ultra-violet photoabsorption cross-sections for nitrosyl chloride and nitryl chloride, *J. Photochem.*, *6*(1), 35–42.

Jenkin, M. E., S. M. Saunders, R. G. Derwent, and M. J. Pilling (1997), World Wide Web site of a Master Chemical Mechanism (MCM) for use in tropospheric chemistry models, *Atmos. Environ.*, *31*(8), 1249.

Jenkin, M. E., K. P. Wyche, C. J. Evans, T. Carr, P. S. Monks, M. R. Alfarra, M. H. Barley, G. B. McFiggans, J. C. Young, and A. R. Rickard (2012), Development and chamber evaluation of the MCM v3. 2 degradation scheme for β-caryophyllene, *Atmos. Chem. Phys.*, *12*(11), 5275–5308, doi:10.5194/acp-12-5275-2012.

Jones, A. R., D. J. Thomson, M. Hort, and B. Devenish (2007), The UK Met Office's next-generation atmospheric dispersion model, in *NAME III. Air Pollution Modeling and Its Application XVII*, edited by C. Borrego and A.-L. Norman, pp. 580–589, Springer, New York.

Keene, W., et al. (1999), Composite global emissions of reactive chlorine from anthropogenic and natural sources: Reactive Chlorine Emissions Inventory, *J. Geophys. Res.*, *104*(D7), 8429–8440, doi:10.1029/1998JD100084.

Kercher, J. P., T. P. Riedel, and J. A. Thornton (2009), Chlorine activation by N_2O_5: Simultaneous, in situ detection of $ClNO_2$ and N_2O_5 by chemical ionization mass spectrometry, *Atmos. Meas. Tech.*, *2*(1), 193–204.

Kim, M. J., D. K. Farmer, and T. H. Bertram (2014), A controlling role for the air-sea interface in the chemical processing of reactive nitrogen in the coastal marine boundary layer, *Proc. Natl. Acad. Sci. U.S.A.*, *111*(11), 3943–3948, doi:10.1073/pnas.1318694111.

Le Breton, M., M. R. McGillen, J. B. A. Muller, A. Bacak, D. E. Shallcross, P. Xiao, L. G. Huey, D. Tanner, H. Coe, and C. J. Percival (2012), Airborne observations of formic acid using a chemical ionisation mass spectrometer, *Atmos. Meas. Tech.*, *4*, 5807–5835, doi:10.5194/amtd-4-5807-2011.

Le Breton, M., et al. (2014a), The first airborne comparison of N_2O_5 measurements over the UK using a CIMS and BBCEAS during the RONOCO campaign, *Anal. Methods*, *6*(24), 9731–9743, doi:10.1039/c4ay02273d.

Le Breton, M., A. Bacak, J. Muller, P. Xiao, B. Shallcross, R. Batt, M. C. Cooke, D. E. Shallcross, S. J.-B. Bauguitte, and C. J. Percival (2014b), Simultaneous airborne nitric acid and formic acid measurements using a chemical ionization mass spectrometer around the UK: Analysis of primary and secondary production pathways, *Atmos. Environ.*, *83*, 166–175, doi:10.1016/j.atmosenv.2013.10.008.

Lidster, R. T., J. F. Hamilton, and A. C. Lewis (2011), The application of two total transfer valve modulators for comprehensive two-dimensional gas chromatography of volatile organic compounds, *J. Sep. Sci.*, *34*, 812–821, doi:10.1002/jssc.201000710.

Manion, J. A., et al. (2014), NIST Chemical Kinetics Database, NIST Standard Reference Database 17, Version 7.0 (Web Version), Release 1.6.8, Data version 2013.03, Natl. Insti. of Standards and Technology, Gaithersburg, Md., 20899–8320. [Available at http://kinetics.nist.gov/.]

Mielke, L. H., A. Furgeson, and H. D. Osthoff (2011), Observation of $ClNO_2$ in a mid-continental urban environment, *Environ. Sci. Technol.*, *45*(20), 8889–8896, doi:10.1021/es201955u.

Mielke, L. H., et al. (2013), Heterogeneous formation of nitryl chloride and its role as a nocturnal NO_x reservoir species during CalNex-LA 2010, *J. Geophys. Res. Atmos.*, *118*, 10–638, doi:10.1002/jgrd.50783.

Nowak, J. B., J. A. Neuman, K. Kozai, L. G. Huey, D. J. Tanner, J. S. Holloway, T. B. Ryerson, G. J. Frost, S. A. McKeen, and F. C. Fehsenfeld (2007), A chemical ionization mass spectrometry technique for airborne measurements of ammonia, *J. Geophys. Res.*, *112*, D10S02, doi:10.1029/2006JD007589.

Osthoff, H. D., et al. (2008), High levels of nitryl chloride in the polluted subtropical marine boundary layer, *Nat. Geosci.*, *1*(5), 324–328, doi:10.1038/ngeo177.

Phillips, G. J., M. J. Tang, J. Thieser, B. Brickwedde, G. Schuster, B. Bohn, J. Lelieveld, and J. N. Crowley (2012), Significant concentrations of nitryl chloride observed in rural continental Europe associated with the influence of sea salt chloride and anthropogenic emissions, *Geophys. Res. Lett.*, *39*, L10811, doi:10.1029/2012GL051912.

Prinn, R. G. (2003), The cleansing capacity of the atmosphere, *Annu. Rev. Environ. Resour*, *28*, 29–57.

Richard, A., et al. (2011), Source apportionment of size and time resolved trace elements and organic aerosols from an urban courtyard site in Switzerland, *Atmos. Chem. Phys.*, *11*(17), 8945–8963, doi:10.5194/acp-11-8945-2011.

Riedel, T. P., et al. (2012), Nitryl chloride and molecular chlorine in the coastal marine boundary layer, *Environ. Sci. Technol.*, *46*, 10,463–10,470, doi:10.1021/es204632r.

Riedel, T. P., et al. (2013), Chlorine activation within urban or power plant plumes: Vertically resolved $ClNO_2$ and Cl_2 measurements from a tall tower in a polluted continental setting, *J. Geophys. Res. Atmos.*, *118*, 8702–8715, doi:10.1002/jgrd.50637.

Riedel, T. P., et al. (2014), An MCM modeling study of nitryl chloride ($ClNO_2$) impacts on oxidation, ozone production and nitrogen oxide partitioning in polluted continental outflow, *Atmos. Chem. Phys.*, *14*, 3789–3800, doi:10.5194/acp-14-3789-2014.

Roberts, J. M., H. D. Osthoff, S. S. Brown, and A. R. Ravishankara (2008), N_2O_5 oxidizes chloride to Cl_2 in acidic atmospheric aerosol, *Science*, *321*(5892), 1059, doi:10.1126/science.1158777.

Roberts, J. M., H. D. Osthoff, S. S. Brown, A. R. Ravishankara, D. Coffman, P. Quinn, and T. Bates (2009), Laboratory studies of products of N_2O_5 uptake on Cl− containing substrates, *Geophys. Res. Lett.*, *36*, L20808, doi:10.1029/2009GL040448.

Rossi, M. J. (2003), Heterogeneous reactions on salts, *Chem. Rev.*, *103*(12), 4823–4882.

Ryerson, T. B., et al. (2013), The 2010 California research at the Nexus of air quality and climate change (CalNex) field study, *J. Geophys. Res. Atmos.*, *118*, 5830–5866, doi:10.1002/jgrd.50331.

Sarwar, G., H. Simon, P. Bhave, and G. Yarwood (2012), Examining the impact of heterogeneous nitryl chloride production on air quality across the United States, *Atmos. Chem. Phys.*, *12*(14), 6455–6473, doi:10.5194/acp-12-6455-2012.

Sarwar, G., H. Simon, J. Xing, and R. Mathur (2014), Importance of tropospheric $ClNO_2$ chemistry across the Northern Hemisphere, *Geophys. Res. Lett.*, *41*, 4050–4058, doi:10.1002/2014GL059962.

Saunders, S. M., M. E. Jenkin, R. G. Derwent, and M. J. Pilling (2003), Protocol for the development of the Master Chemical Mechanism, MCM v3 (Part A): Tropospheric degradation of non-aromatic volatile organic compounds, *Atmos. Chem. Phys.*, *3*(1), 161–180, doi:10.5194/acp-3-161-2003.

Simmons, A. J., and D. M. Burridge (1981), An energy and angular-momentum conserving vertical finite-difference scheme and hybrid vertical coordinates, *Mon. Weather Rev.*, *109*(4), 758–766.

Simon, H., Y. Kimura, G. McGaughey, D. T. Allen, S. S. Brown, H. D. Osthoff, J. M. Roberts, D. Bun, and D. Lee (2009), Modeling the impact of $ClNO_2$ on ozone formation in the Houston area, *J. Geophys. Res.*, *114*, D00F03, doi:10.1029/2008JD010732.

Simpson, W. R., et al. (2007), Halogens and their role in polar boundary-layer ozone depletion, *Atmos. Chem. Phys.*, *7*(16), 4375–4418, doi:10.5194/acp-7-4375-2007.

Slusher, D. L., G. Huey, and D. J. Tanner (2004), A thermal dissociation-chemical ionization mass spectrometry (TD-CIMS) technique for the simultaneous measurement of peroxyacyl nitrates and dinitrogen pentoxide, *J. Geophys. Res.*, *109*, D19315, doi:10.1029/2004JD004670.

Spicer, C. W., E. G. Chapman, B. J. Finlayson-Pitts, R. A. Plastridge, J. M. Hubbe, J. D. Fast, and C. M. Berkowitz (1998), Unexpectedly high concentrations of molecular chlorine in coastal air, *Nature*, *394*(6691), 353–356, doi:10.1038/28584.

Stevenson, D. S., C. E. Johnson, W. J. Collins, R. G. Derwent, K. P. Shine, and J. M. Edwards (1998), Evolution of tropospheric ozone radiative forcing, *Geophys. Res. Lett.*, *25*(20), 3819–3822, doi:10.1029/1998GL900037.

Stone, D., et al. (2010), HO_x observations over West Africa during AMMA: Impact of isoprene and NO_x, *Atmos. Chem. Phys.*, *10*(19), 9415–9429, doi:10.5194/acp-10-9415-2010.

Tham, Y. J., C. Yan, L. Xue, Q. Zha, X. Wang, and T. Wang (2014), Presence of high nitryl chloride in Asian coastal environment and its impact on atmospheric photochemistry, *Chin. Sci. Bull.*, *59*(4), 356–359.

Thornton, J. A., et al. (2010), A large atomic chlorine source inferred from mid-continental reactive nitrogen chemistry, *Nature*, *464*(7286), 271–274, doi:10.1038/nature08905.

Visser, S., et al. (2014), Kerb and urban increment of highly time-resolved trace elements in PM10, PM2.5 and PM1.0 winter aerosol in London during ClearfLo 2012, *Atmos. Chem. Phys. Discuss.*, *14*(11), 15,895–15,951, doi:10.5194/acpd-14-15895-2014.

Wang, X., T. Wang, C. Yan, Y. J. Tham, L. Xue, Z. Xu, and Q. Zha (2014), Large daytime signals of N_2O_5 and NO_3 inferred at 62 amu in a TD-CIMS: Chemical interference or a real atmospheric phenomenon?, *Atmos. Meas. Tech.*, *7*(1), 1–12.

Wayne, R. P., et al. (1991), The nitrate radical: Physics, chemistry, and the atmosphere, *Atmos. Environ. Part A*, *25*(1), 1–203, doi:10.1016/0960-1686(91)90192-A.

Whalley, L. K., et al. (2010), The chemistry of OH and HO_2 radicals in the boundary layer over the tropical Atlantic Ocean, *Atmos. Chem. Phys.*, *10*, 1555–1576, doi:10.5194/acp-10-1555-2010.

Wilkins, R. A., Jr., M. C. Dodge, and I. C. Hisatsune (1974), Kinetics of nitric oxide catalyzed decomposition of nitryl chloride and its related nitrogen isotope exchange reactions, *J. Phys. Chem.*, *78*(21), 2073–2076, doi:10.1021/j100614a001.

Young, C. J., et al. (2012), Vertically resolved measurements of nighttime radical reservoirs in Los Angeles and their contribution to the urban radical budget, *Environ. Sci. Technol.*, *46*(20), 10,965–10,973, doi:10.1021/es302206a.

Young, D. E., J. D. Allan, P. I. Williams, D. C. Green, M. J. Flynn, R. M. Harrison, J. Yin, M. W. Gallagher, and H. Coe (2014), Investigating the annual behaviour of submicron secondary inorganic and organic aerosols in London, *Atmos. Chem. Phys. Discuss.*, *14*(13), 18,739–18,784, doi:10.5194/acpd-14-18739-2014.